DC VOLTAGE CONTROL IN OFF-SHORE WIND FARMS WITH DISTRIBUTED DIODE RECTIFIER UNITS

G. Chaqués-Herraiz, S. Bernal-Perez, J. Martínez-Turégano, S. Añó-Villalba, R. Peña, R. Blasco-Gimenez
Universitat Politècnica de València, Spain (r.blasco@ieee.org)

***Abstract*—Distributed diode rectifier units have been proposed as a robust and cost efficient solution for the connection of large off-shore wind farms to HVDC links. However, since the diode rectifier platforms are connected in series with cables of varying distances, their dc-side voltage might not be the same in all diode rectifier platforms. This paper introduces a diode rectifier platform dc-voltage balancing control to cancel the aforementioned unbalanced. Balanced operation has been shown by means of detailed PSCAD simulations, considering a wide range of power generation unbalance between the wind power plants connected to the HVDC diode rectifier platforms. Moreover, the proposed balancing control has shown a very good dynamic performance.**

***Index Terms*—HVDC diode rectifier, HVDC link control, HVDC grid, off-shore wind power plant, Multiterminal**

I. Introduction

OFFSHORE wind energy resources in Europe need network infrastructure to evacuate the power produced to on-shore grids. HVDC links have been preferred to HVAC links when distance to the shore is longer than 80 km, as they have been proved to be the most cost-effective solution. Multiterminal HVDC transmission is expected to play a key role in future power grids. However, these HVDC offshore grids are currently facing several challenges: network restoration issues, compliance with grid codes and control strategies to ensure the power flow inside the network [1].

Diode-based rectifiers for unidirectional HVdc links have been suggested in the past as an alternative to increase efficiency and system reliability [2], [3]. Specifically, diode rectifiers have been proposed for the connection of single unit generators to HVdc grids with Line Commutated Converters (LCC) in order to achieve reduced losses, decreased complexity and enhanced reliability [4]. Moreover, diode rectifiers have been proposed as a technical solution for the grid access of large off-shore wind farms [5]. However, this new technology must overcome the same challenges mentioned for HVDC grids, finding its own specific solutions.

Previous work by the authors' has shown that a diode-based HVdc rectifier is a feasible solution for the point-to-point connection of large off-shore WPP using inverter stations based on Line Commutated Thyristors (LCT) [6], [7] or on Voltage Source Converters (VSCs) [8]. HVDC diode rectifiers (DRs) have also been included in an hybrid multiterminal system combining DRs and VSC converters to connect wind power plants to on-shore grids. This paper studies the topology proposed in [5], where three diode rectifier platforms, consisting on two 24-pulse diode rectifier each, have their dc-sided connected in series and their ac-sides connected in parallel by means of a ring bus. Each one of the platform is close to a connecting off-shore wind farm, thus reducing the number of platforms required for the HVDC connection of three large wind farms from 4 to 3 [5]. By using a 66kV off-shore ac-grid, this topology combines the advantages of HVDC and HVAC connection.

In this topology, however, different active power delivered by each wind turbine, together with cable impedances, might lead to different ac and dc voltage magnitudes on each DR platform. This paper includes a balancing controller in order to provide equal dc-side voltages for each DR platform.

The proposed control algorithm has been validated by considering a system with three Wind Power Plants (WPPs), considered as a aggregated models, connected to a radial HVAC and a DR converter each. Droop control has been used for the primary frequency and voltage control of each wind turbine [9]. A higher level control has been introduced to balance the $E_{Rdc,i}$ voltages of the diode rectifier platforms.

The proposed control strategies are validated by means of detailed PSCAD/EMTDC simulation considering open and closed ring bus connection between the diode rectifier platforms in quasi-steady state and transient operation, considering both open and closed ac-ring bus.

II. System Description and Control

A. Modeling

The proposed system is shown in Fig. 1. It represents three off-shore WPP connected to an on-shore grid through a diode based HVDC link [5].

Each WPP consist of 50 WTs rated at 8 MW each one, therefore each WPP is rated at 400 MW, adding up to a total 1.2 GW. The considered wind turbines (WTs) are type-4 WTs, so their generators are connected to the off-shore AC grid through a full scale back-to-back converter, a PWM filter and a WT transformer ($T_{WT,i}$). An aggregated model is used to represent each one of the Wind Power Plants.

The diode rectifier (DR) station consists of three different platforms. Each WPP connects to the nearest DR platform at bus $V_{F,i}$. The three PCC buses are connected to an ac ring-bus to allow for redundancy againgst cable and DR station faults.

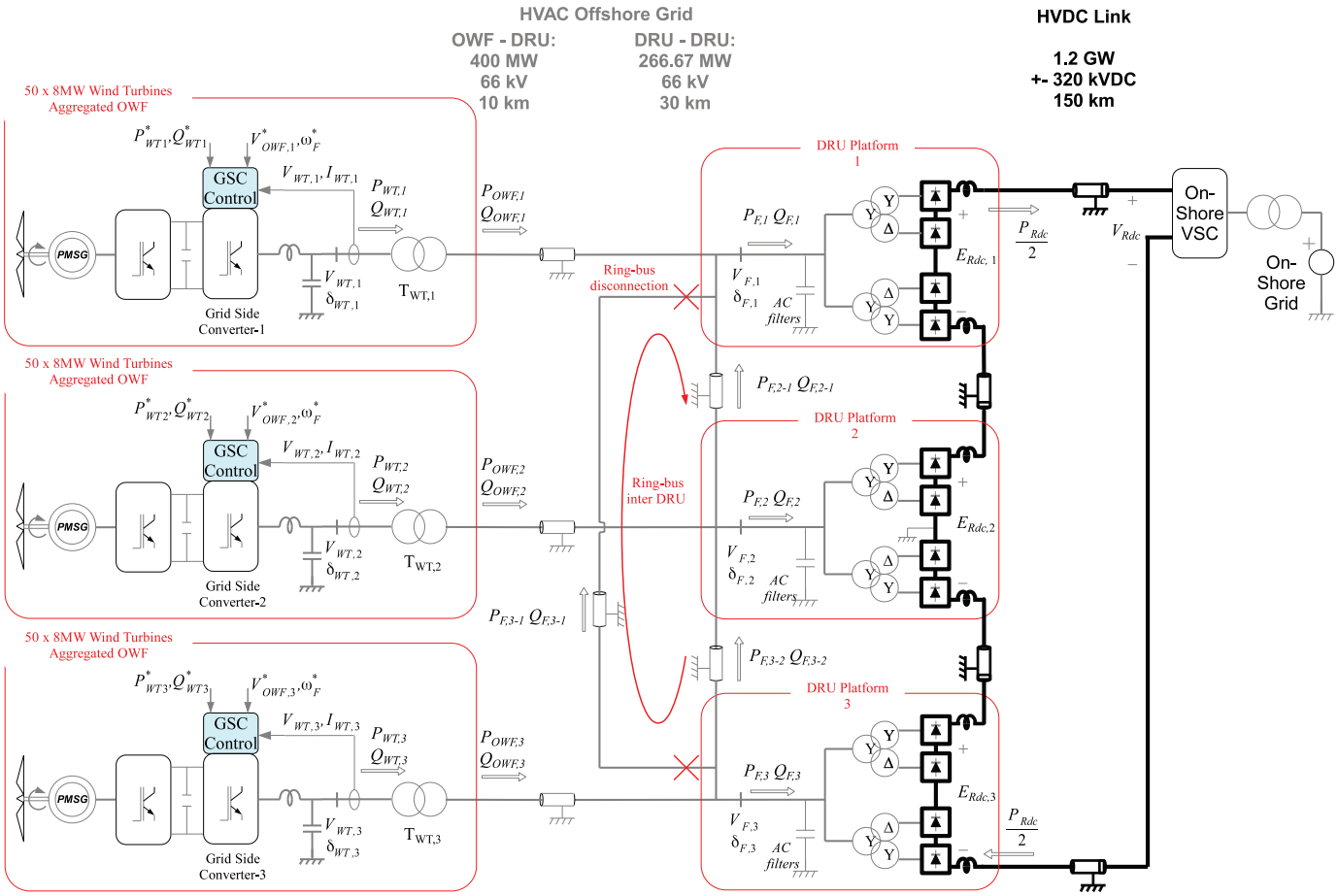

Fig. 1. Wind Power Plant (WPP) offshore AC Grid model

The parameters of the Π model used for the submarine cable linking the WPPs to their respective PCCs have been taken from manufacturer catalogues and are included in the appendix as HVAC Cable 1. HVAC Cable 2 corresponds to the ring bus connecting the platforms.

Each DR platform has two 12-pulse diode rectifier units, together with their corresponding rectifier transformer and ac filters. The diode rectifiers are connected in series at the HVDC side. Finally, the on-shore VSC converter is assumed to operate in dc-side voltage control mode and has been modelled as an equivalent dc-source.

B. Offshore AC grid control

Since rectifiers are uncontrolled, AC off-shore grid power control has to be carried out completely by the WT Grid Side Converters (GSCs). AC offshore grid is mainly inductive and its power flow ($P_{WT,i}, P_{F,i-j}$) can be controlled by phase differences ($\delta_{WT,i}, \delta_{F,i}$). Therefore, off-shore ac-grid frequency and voltage control has been carried out by using standard $P-\omega$, $Q-V$ droop control [9].

Conversely, the power flow through rectifiers ($P_{F,i}$) has very little frequency relation and is controlled by the AC side voltage magnitude ($V_{F,i}$). Clearly, considering the steady state average characteristic of the diode rectifier:

$$E_{Rdc,i} = \frac{3\sqrt{6}}{\pi} B N V_{F,i} - \frac{3}{\pi} B \omega_F L_{TR} I_{Rdc} \qquad (1)$$

the diode rectifier dc-side voltage $E_{Rdc,i}$ is almost proportional to the corresponding ac-side voltage $V_{F,i}$, with the term $-\frac{3}{\pi} B \omega_F L_{TR}$ acting as a resistive term in series with the HVDC cable. Therefore, the overall ac-grid voltage magnitude is used to control the total power flow through the HVDC link via the Diode Rectifier stations.

The overall control diagram is shown in Fig. 2. It is divided in three levels: OWF Central Controller, OWF-i Controller and WT GSC Controller in every single WT.

The first one is centralised and controls the total HVDC power flow. It receives reference and measured active powers from Off-shore Wind Farm (OWF) Controllers, computes the total power that should be delivered to the HVDC Link and changes the WPP voltage references in order to set it.

The proposed $E_{Rdc,i}$ compensator block is included at this level, in order to keep rectifier DC side voltages balanced even with different active powers being generated by individual Wind Power Plants. This feature will be discussed in detail in the following subsection.

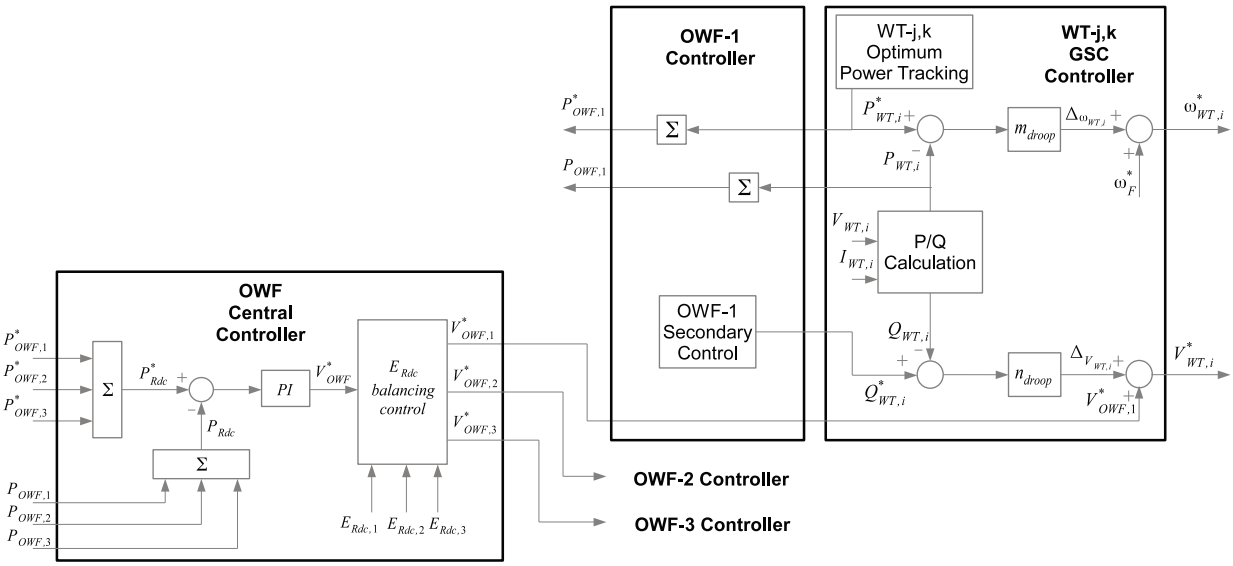

Fig. 2. WPP power generation control structure

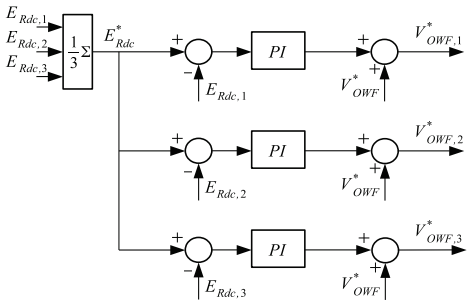

Fig. 3. E_{Rdc} balancing controller

The second control level is related to each OWF controller. On the one hand it receives reference and measured active powers ($P^*_{WT,i}, P_{WT,i}$) from WT Controllers and computes the total power that should be delivered by the OWF. On the other hand, it sends the corresponding OWF voltage reference ($V^*_{OWF,i}$) to each one of the local WT controllers and optimize the reactive power flow within the OWF.

The third control level is the local controller of each WT. The optimum power tracking algorithm calculates the optimal active power reference, ${P_{WT,i}}^*$, that can be extracted for each particular operating condition (wind speed, rotor speed,...) [10].

Finally, each WT GSC acts as a grid forming converter by implementing classical $P-\omega$, $Q-V$ droop control in order to share their active and reactive power contributions [9]. Active and reactive power are measured at the low voltage WT transformer winding and then filtered with a first order filter ($\omega_c = 10$ Hz) to obtain the mean value. The droop block sets WT voltage magnitude and frequency that is sent to the GSC.

C. DC Voltage balancing control

DC side converter voltages, $E_{Rdc,i}$, should be kept balanced in order to have equal power flow through each Diode Rectifier station ($P_{F,i}$). Moreover, since the total HVDC voltage (V_{Rdc}) is kept at its nominal value by the on-shore VSC, the fact that $E_{Rdc,i}$ are not balanced implies that at least one of the diode rectifier stations is above its nominal value. Clearly, if an unbalance correction mechanism is not used, then the complete system must be slightly de-rated.

Therefore, a centralised DC voltage balancing control is proposed (Fig. 3). The voltage balancing control takes the average E^*_{Rdc} voltage as an input:

$$E^*_{Rdc} = \frac{1}{3}\sum_i E_{Rdc,i} \tag{2}$$

Then individual PI controllers add a term to the overall voltage reference used in each wind farm $Q-V$ primary droop control ($V^*_{OWF,1,2,3}$).

III. Results

The proposed dc-side voltage balancing strategy is validated in this section by means of EMT PSCAD simulations.

Two cases are presented to compare the proposed controller contribution:

A. Quasi-steady state DRU behaviour, without DRU voltage balancing control.
B. Quasi-steady state DRU behaviour, with DRU voltage balancing control.

Finally, a third case shows the corrective actions that yields to a balanced DC voltage distribution. The system starts at the worst case scenario without balancing control and, at a certain time, the proposed control is enabled.

Each case is also further in two subcases in order to illustrate the effects of ring-bus connection availability, i.e. with full

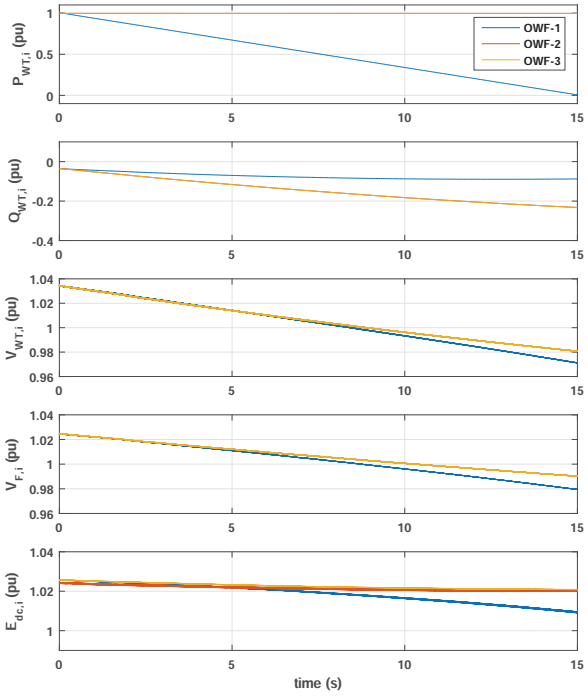

Fig. 4. OWF-1 power ramp down with no $E_{Rdc,i}$ balancing control

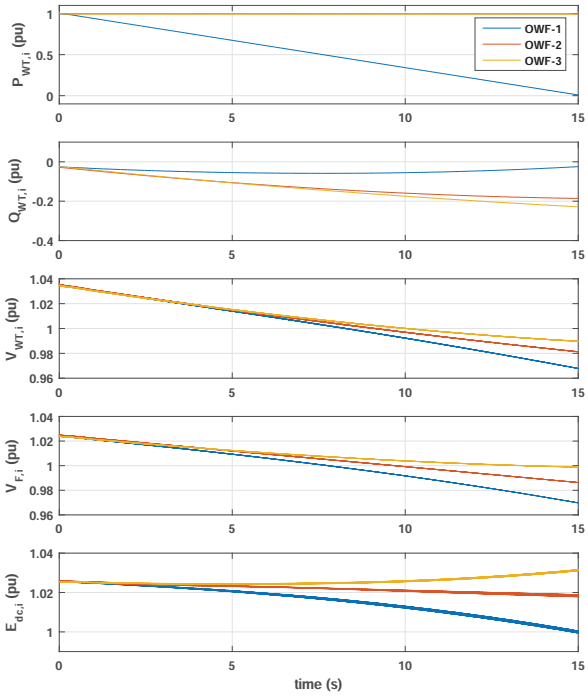

Fig. 5. OWF-1 power ramp down with no $E_{Rdc,i}$ balancing control and no DRU_1-DRU_3 ring bus connection

and with open ac-ring bus connection (see Fig. 1). The latter subcase implies a larger voltage unbalance and hence needs to be considered as it represents the worst case scenario.

A. Quasi-steady state DRU operation without voltage balancing

1) Ring-bus connected: Fig. 4 shows power flow and voltage magnitudes of the off-shore AC grid when OWF power generation becomes unbalanced. In this case, the power delivered by OWF-1 is ramped down to illustrate the $E_{Rdc,i}$ voltage unbalance that appears when all OWFs are not generating the same active power.

The top trace shows the active power delivered by each OWF ($P_{WT,i}$). Initially, all Off-shore Wind Farms are generating their rated active power. Then, OWF-1 active power is ramped down while $P_{WT,2}$ and $P_{WT,3}$ are kept at their nominal value.

The second trace shows the reactive power delivered by each OWF ($Q_{WT,i}$). As the active power through the diode rectifiers is reduced, and so is its reactive power demand, there is a reactive power overcompensation by the Diode Rectifier ac-filters. Therefore, the off-shore wind farms need to absorb the additional reactive power and hence ($Q_{WT,i}$) increased.

Moreover, the OWFs reactive surplus consumption is not balanced: OWF-1 absorbs less reactive power than the other two due to the nature of the droop controllers used within the wind turbines.

The third trace shows the voltages at the OWF terminals ($V_{WT,i}$). Clearly, these voltages are decreased by the centralised power control in order to reduce total HVDC power transmission ($P_{Rdc,i}$).

The fourth trace shows that the ac voltages at the points of common coupling of each OWF ($V_{F,i}$) show a similar behaviour to the OWF terminal voltages, becoming unbalanced as the active power of OWF-i is reduced to zero. Different $V_{F,i}$ voltages clearly lead to different $E_{Rdc,i}$ voltages, as per (1).

Worst case voltage unbalance between diode rectifier stations occurs with OWF-i active power is zero. At this stage, $\Delta V_F \approx \Delta E_{Rdc} \approx 1\%$.

2) Ring-bus not connected: Fig. 5 shows the same case as that in Fig. 4, i.e. OWF-1 active power reduction, but now assuming that there is no ring bus connection between DRU-1 and DRU-3.

Clearly, active power generation ($P_{WT,i}$) is properly controlled: OWF-1 is ramped down while $P_{WT,2}$ and $P_{WT,3}$ are kept at their nominal value.

The rest of the traces clearly illustrate the effect of having an open ac-ring bus. Comparing figs. 5 and 4, with an open ring bus, there are larger unbalances on the reactive power absorbed by each OWF ($P_{WT,i}$), on OWF and PCC voltages ($V_{WT,i}$ and $V_{F,i}$, respectively) and hence on diode rectifier dc-side voltages ($E_{Rdc,i}$).

In this case, maximum $E_{Rdc,i}$ unbalance is $\Delta E_{Rdc} \approx 3\%$

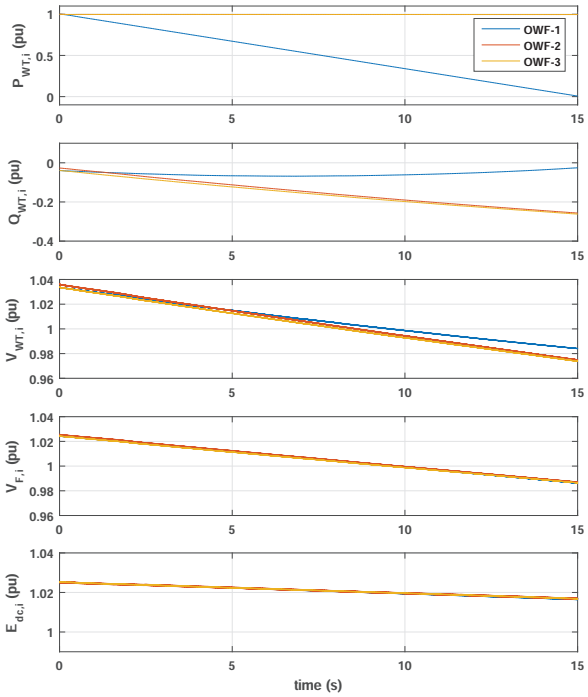

Fig. 6. $OWF-1$ power down with E_{dc} balancing control

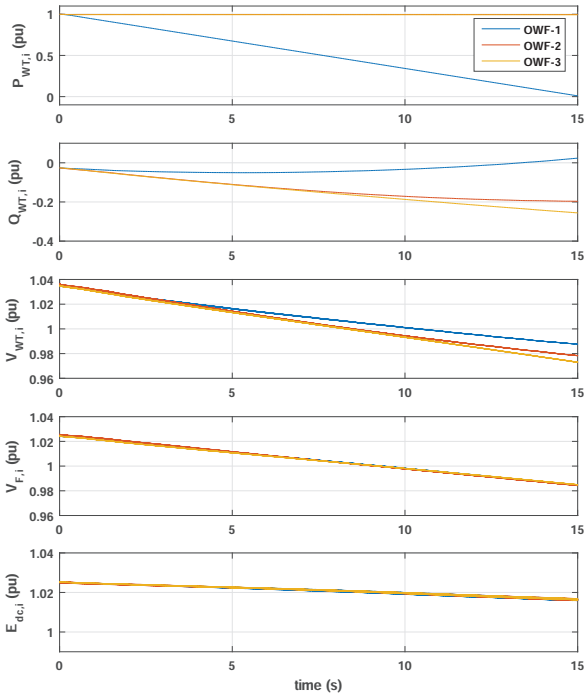

Fig. 7. $OWF-1$ power down with E_{dc} balancing control and no DRU_1-DRU_3 ring bus connection

B. Quasi-steady state DRU voltage balancing control

In this section, the proposed voltage balancing strategy is validated considering the quasi-steady state transients shown in the previous section, with closed (fig. 4) and open (fig. 5) ring bus.

1) Closed ring-bus: Fig. 6 shows the same case as that in fig. 4, i.e. ramp down of the active power delivered by OWF-1 ($P_{WT,1}$), but now with the E_{Rdc} voltage balancing control shown in fig. 3 enabled.

As expected, active power generation is not influenced by the balancing controller. However, reactive power flow has changed compared to fig. 4. Moreover, the balancing controller adjusts the individual OWF voltage references so ac voltage magnitudes at $V_{F,1}$, $V_{F,2}$ and $V_{F,3}$ are equal and therefore $E_{Rdc,1}$, $E_{Rdc,2}$ and $E_{Rdc,3}$ are also equal as per (1). I.e. $\Delta V_F = \Delta E_{Rdc} = 0$.

2) Ring-bus not connected: Fig. 7 shows that the proposed DRU voltage balancing control mitigates unbalanced DC voltages even if ring bus is not operational. Active power is again properly controlled while reactive power flow has changed compared to that in Fig. 7: OWF-1 consumption is lower and OWF-2,3 reactive power consumptions are somehow larger.

Voltage compensation is no longer equal in OWF-2 and OWF-3 because of the absence of the ring-bus connection. In spite of a larger reactive power unbalance between WPPs, voltages $V_{F,1}$, $V_{F,2}$ and $V_{F,3}$ are controlled at to have the same magnitude and hence $\Delta V_F = \Delta E_{Rdc} = 0$.

Therefore, the proposed control system shows a good performance for a wide range of active power generation unbalance amongst WPPs even when the ac-ring bus is open.

C. DRU voltage balancing control activation

1) Ring-bus not connected: Fig. 8 shows the behaviour of the complete system when the $E_{Rdc,i}$ voltage balancing control is activated, considering an open ac-ring bus.

Initially, power generation is set to the worst case scenario, i.e. $P_{WT,1} = 0$; $P_{WT,2} = P_{WT,3} = 1pu$). Therefore, the active power flowing through DRU-1 needs to be fed by OWF-2 and OWF-3.

at $t = 0$, fig. 8 shows a 3% voltage unbalance between both ac-grid PCC voltages ($V_{F,i}$) and diode rectifier dc-side voltages ($E_{Rdc,i}$).

At $t = 2$s, $E_{Rdc,i}$ voltage balancing control is enabled. The controller changes the magnitude of OWF voltage references to compensate the unbalanced DC voltages. The reactive power contribution of each wind farm ($Q_{WT,i}$) is changed by the $E_{Rdc,i}$ balancing control so $\Delta V_F = \Delta E_{Rdc} = 0$ in about 200 ms.

Active power generation of each wind farm follows their respective constant references since the WT $P-\omega$ droop controller sets the GSCs voltage phase differences independently of the reactive power injected by each individual WPP.

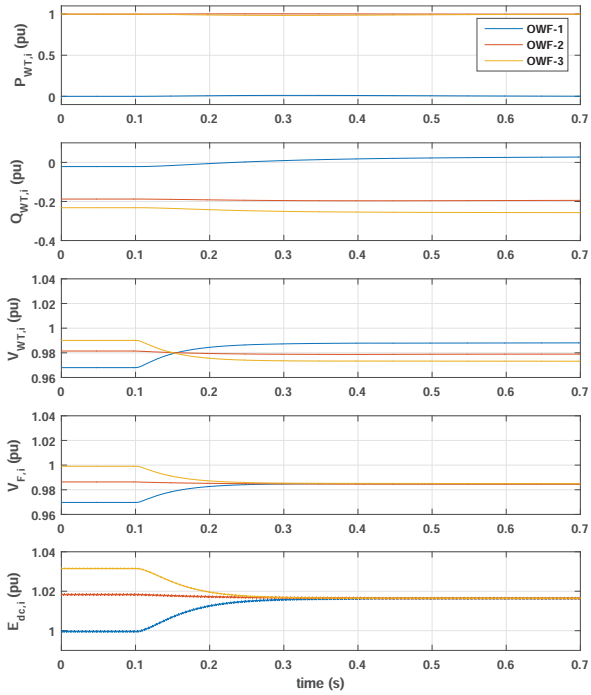

Fig. 8. E_{Rdc} balancing controller activation under unbalanced generation

IV. Discussion and Conclusions

This paper has shown that series connected Diode Rectifier Stations show uneven HVDC voltage sharing when the active power generated by different off-shore wind farms is different.

The paper has proposed a balancing control which modifies the voltage reference at the PCC of each wind power plant, leading to equal DRU terminal ac voltage magnitudes (V_{Fi}) and hence to equal sharing of HVDC voltage amongst Diode Rectifier Units ($E_{Rdc,i}$). The proposed strategy has been validated using detailed PSCAD simulations on a realistic scenario.

The proposed balancing mechanism has shown adequate performance for a wide range of generated power differences between wind power plants. Moreover, its performance is not affected when the ac ring bus connecting the DRU platforms is open.

This paper has also shown that the proposed $E_{Rdc,i}$ balancing strategy is capable of cancelling DRU DC-side voltages differences in less than a second.

Acknowledgments

The authors would like to thank the support of the Spanish Ministry of Economy and EU FEDER Funds under grant DPI2014-53245-R, and the support of CONICYT (Chile) under grants FONDAP/15110019 and Fondecyt 1151325.

This project has received funding from the *European Unionś Horizon 2020 research and innovation program* under grant agreement No. 691714.

Appendix

Aggregated Wind Turbines		
Front-end: 1.2 kVcc, 690 kVac, 50 Hz		
PWM filter: R_T = 0.008 p.u.; L_T = 0.18 p.u.; C_T = 20 p.u.		
Transformer T_R: 8 MVA, 50 Hz, 0.69/66 kV (L-L rms), X_L = 0.18 pu		
Transformer T_{Wi}: 0.69/66 kV	$R_{Wi} = 0.005$ pu	$L_{Wi} = 0.08$ pu
HVac Cable 1 Π-model (8 x 10 km)		
C_H = 2 x 7.2 μF	$L_H = 0.5375$ mH	$R_H = 0.1875\ \Omega$
HVac Cable 2 Π-model (3 x 30 km)		
C_H = 2 x 3.9 μ F	$L_H = 10.5$ mH	$R_H = 1.1\ \Omega$
HVdc Rectifier (based on Cigre benchmark model)		
Capacitor Bank: $C_F = 24.1144\ \mu$F		
ZF-low frequency filter		
$C_{a1} = 48.236\ \mu$F	$C_{a2} = 535.9714\ \mu$F	$L_a = 18.9036$ mH
$R_{a1} = 4.1244\ \Omega$	$R_{a2} = 36.2924\ \Omega$	
ZF-high frequency filter		
$C_b = 48.236\ \mu$F	$R_b = 11.547\ \Omega$	$L_b = 1.8848$ mH
Transformer $T_{R\Delta}$ and T_{RY}		
66/40.41 kV, 240 MVA	$L_{R,lk} = 0.18$ pu	$L_{R,m} = 0.01$ pu
dc-smoothing reactor: $L_R = 0.033$ H		
PI Controller Parameters		
PI Power Controller:	$K_P = 0.00006$	$T_I = 380$
Proportional frecuency droop:	$m_P = 0.01$ Ws/rd	
Proportional amplitude droop:	$n_P = 0.01$ Var/V	

References

[1] L. jie Zhao, H. Rao, X. lin Li, W. Zhang, Y. Xiang, and M. li Fu, "Development of ±160 kv xlpe cable and its application to the world's first three-terminal vsc hvdc system in china," in *CIGRE AORC Technical Meeting, B1-1110*, 2014, pp. 1–7.

[2] T. Machida, I. Ishikawa, E. Okada, and E. Karasawa, "Control and protection of HVDC systems with diode valve converter," *Electrical Engineering in Japan*, vol. 98, no. 1, pp. 62–70, Jan. 1978. [Online]. Available: http://onlinelibrary.wiley.com/doi/10.1002/eej.4390980109/abstract

[3] S. Hungsasutra and R. M. Mathur, "Unit connected operator with diode valve rectifier scheme," *IEEE Transactions on Power Systems*, vol. 4, no. 2, pp. 538–543, May 1989.

[4] J. Bowles, "Multiterminal HVDC transmission systems incorporating diode rectifier stations," *Power Apparatus and Systems, IEEE Transactions on*, vol. PAS-100, no. 4, pp. 1674–1678, Apr. 1981.

[5] P. Menke, "New Grid Access Solution for offshore wind farms," in *EWEA OFFSHORE 2015*, 2015. [Online]. Available: http://proceedings.ewea.org/offshore2015/conference/programme/info2.php?id2=225&id=26%20&ordre=9

[6] R. Blasco-Gimenez, S. Añó-Villalba, J. Rodriguez-D'Derlée, S. Bernal-Pérez, and F. Morant, "Diode-Based HVdc link for the connection of large offshore wind farms," *IEEE Transactions on Energy Conversion*, vol. 26, no. 2, pp. 615–626, Jun. 2011.

[7] R. Blasco-Gimenez, S. Añó-Villalba, J. Rodríguez-D'Derlée, F. Morant, and S. Bernal-Perez, "Distributed Voltage and Frequency Control of Offshore Wind Farms Connected With a Diode-Based HVdc Link," *IEEE Transactions on Power Electronics*, vol. 25, no. 12, pp. 3095–3105, Dec. 2010.

[8] S. Bernal-Perez, S. Añó-Villalba, R. Blasco-Gimenez, and J. Rodríguez-D'Derlée, "Off-shore wind farm grid connection using a novel diode-rectifier and VSC-inverter based HVDC transmission link," in *IECON 2011 - 37th Annual Conference of the IEEE Industrial Electronics Society*, Nov. 2011, pp. 3186–3191.

[9] J. M. Guerrero, J. C. Vasquez, J. Matas, L. G. De Vicuña, and M. Castilla, "Hierarchical control of droop-controlled AC and DC microgridsA general approach toward standardization," *IEEE Transactions on Industrial Electronics*, vol. 58, no. 1, pp. 158–172, 2011. [Online]. Available: http://ieeexplore.ieee.org/xpls/abs_all.jsp?arnumber=5546958

[10] E. Muljadi and C. P. Butterfield, "Pitch-controlled variable-speed wind turbine generation," *IEEE Transactions on Industry Applications*, vol. 37, no. 1, pp. 240–246, Jan. 2001.